Application of Artificial Neural Networks for Estimation of the Reaction Rate in Methanol Dehydration

ARTICLE *in* INDUSTRIAL & ENGINEERING CHEMISTRY RESEARCH · APRIL 2010

Impact Factor: 2.59 · DOI: 10.1021/ie9020705

Application of Artificial Neural Networks for Estimation of the Reaction Rate in Methanol Dehydration

Peyvand Valeh-e-Sheyda,*,† Fereydoon Yaripour,‡ Gholamreza Moradi,† and Mohammad Saber§

Catalyst Research Center, Department of Chemical Engineering, Faculty of Engineering, Razi University, Kermanshah, Iran, Catalyst Research Group, Petrochemical Research and Technology Company, National Petrochemical Company, 14358 Tehran, Iran, and Department of Energy Engineering, Sharif University of Technology, Tehran, Iran

In this paper, the artificial neural network has been applied to estimate the reaction rate of methanol dehydration in dimethyl ether synthesis. The multilayer feed forward neural network with three inputs and one output has been trained with different algorithms and different numbers of neurons in the hidden layer. Two thirds of all training data are used for training of the network and the rest are used for testing of the generalization of the network. The accuracy of the proposed model was found to agree well with the experimental results over a wide range of experimental conditions. The results clearly depict that the neural network is a powerful tool to estimate the reaction rate and the designed neural network can be used instead of approximate and complex analytical equations.

1. Introduction

Synthesis of new liquid fuels and other hydrocarbon products from coal, natural gas, or biomass is becoming an area of both academic and industrial activity. Among those products, dimethyl ether (DME) has received global attention during the past few years because it is not only a clean fuel but also an excellent propellant, refrigerant, and important feedstock for the preparation of light alkenes.[1−4]

DME can be synthesized via dehydration of methanol (MeOH) over solid acid catalysts such as modified-alumina, γ-alumina (γ-Al_2O_3), zeolite, or ion-exchange resins in a temperature range of 453−673 K and at pressures of up to 18 bar[5−9] according to the following reaction:

$$2CH_3OH \Leftrightarrow DME + H_2O \quad (1)$$

The intrinsic kinetics of MeOH dehydration was investigated quantitatively in a multitude of studies; many of them have been offered rate expressions based on Eley−Rideal[10] or Langmuir−Hinshelwood theories.[11−14] It is still quite difficult to identify a classical kinetic expression of the dehydration process to estimate the reaction rate because of complexity of equations and the temperature dependence of the chemical equilibrium constant. Furthermore, discrimination of the kinetic models and estimation of the kinetic parameters for the kinetic model do not always exhibit very good accuracy with experimental data. A number of published works are dedicated to investigation of the kinetics of this process on different solid acid catalysts. As investigated by Pop et al.,[4] a published rate expression with a correlation coefficient, $R^2 = 0.967$, was adapted to describe the experimentally observed process kinetics over an H-SAPO-34 molecular sieve. Lee et al.[13] derived a kinetic equation with $R^2 = 0.972$ between experimentally measured and calculated rates on the γ-Al_2O_3 catalyst. However, in other studies, the accuracy of statistical criteria was not reported clearly.

The present work investigates the possibility and capability of using the artificial neural network (ANN) to estimate the reaction rate by taking MeOH conversion over commercial γ-Al_2O_3 as an example. The authors believe that investigation of the intrinsic kinetic modeling of the DME reactor using the ANN has never been published in open literature.

It is worthwhile to say that the ANN is a powerful mathematical modeling tool especially for complex systems with no need for the complex equations governing the system. The capability of learning from experimental data and simplicity of implementation are the advantages of the ANNs over the classic kinetic modeling methods.

Because the multilayer feed forward neural network is the most commonly used network for the function approximation problem as well as its strong learning capability, it has been used in this study.

2. Experimental Section

2.1. Catalyst Preparation. Because γ-Al_2O_3 catalyst has been extensively used for the production of DME from MeOH dehydration,[14−16] a commercial γ-Al_2O_3 catalyst prepared by Catalyst Research Group of Iranian Petrochemical Research and Technology has been chosen for this process. Samples were crushed and sieved to sizes 90−125 μm, and then they were activated via a heating rate of 5 K/min under N_2 flow (50 mL/min) at 493 K for 2 h under atmospheric pressure.

2.2. Characterizations. A N_2 adsorption experiment was carried out over a NOVA 2000 series instrument (Quantachrome Instruments, Boynton Beach, FL) at liquid-N_2 temperature (77 K), and the surface area and pore distribution of the samples were calculated according to Brunauer−Emmett−Teller (BET) and Barret−Joyner−Halenda methods, respectively. Prior to analysis, 250 mg of the catalyst was degassed at 250 °C for 16 h under flowing N_2.

The X-ray diffraction (XRD) pattern of the sample was recorded on an X-ray diffractometer (Philips PW-1800) using a Cu Kα monochromatized radiation source and a Ni filter in the 2θ range of 5−90°.

The acidity of the sample was measured via ammonia temperature-programmed desorption (NH_3-TPD) using a TPR/

* To whom correspondence should be addressed. E-mail: peyvand_vs@yahoo.com.
† Razi University.
‡ National Petrochemical Company.
§ Sharif University of Technology.

10.1021/ie9020705
Published on Web 04/20/2010

Table 1. Physical Properties of the Fresh γ-Al_2O_3 Catalyst

catalyst name	multipoint BET (m^2/g)	single-point BET (m^2/g)	total pore volume (mL/g)	average pore radius (Å)
γ-Al_2O_3	108.84	102.89	0.066	12.10

TPD 2900 instrument (Micromeritics, Norcross, GA) with a conventional flow apparatus included with an online thermal conductivity detector (TCD). In a typical analysis, NH_3-TPD was performed using 0.35 g of the catalyst, which was degassed at 600 °C in a helium flow, cooled to 150 °C, and then saturated with NH_3 for 15 min. After saturation, the sample was purged with He for 30 min to remove weakly adsorbed NH_3 on the surface of the catalyst. During this time, a constant TCD level was attained. The temperature of the sample was then raised at a heating rate of 5 °C/min from 150 to 700 °C, and the amount of ammonia in the effluent was measured via TCD and recorded as a function of the temperature.

2.3. Catalyst Characterizations. Table 1 summarizes the specific BET surface area, total pore volume, and average pore radius of the fresh catalyst that has been used for experiments.

The XRD analyses of the fresh catalyst (Figure 1) indicate that the catalyst is highly amorphous in nature, with a low level of crystallinity in the form of cubic aluminum oxide (JCPDS No. 79-1558).

The NH_3-TPD method was used to investigate the acid properties of the alumina sample, and the results are depicted in Figure 2. Desorption peaks with maxima in the ranges of 180−280, 290−350, and 360−600 °C in the NH_3-TPD pattern are commonly ascribed to the ammonia desorbed from the weak and strong acid sites, respectively.[17]

The NH_3-TPD spectra of γ-Al_2O_3 show two maximum peaks at 324 and 829 °C corresponding to medium and strong acid sites, respectively. According to the results, the area under the first peak is larger than that under the second peak. This observation means that the number of moderate acid sites is greater than the number of strong acid sites for this sample. That is why the high catalytic performance for dehydration of methanol (MeOH) over the γ-Al_2O_3 commercial sample can be assigned to the amount of medium Brønsted acid sites.

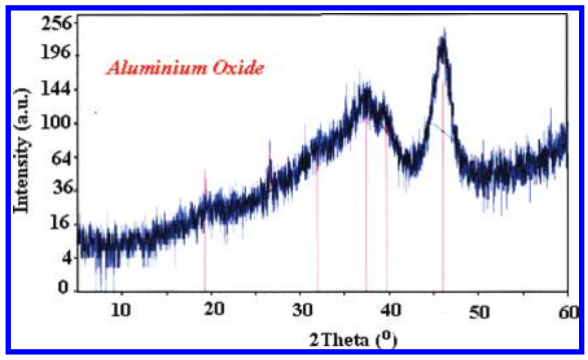

Figure 1. Powder XRD pattern for a commercial γ-Al_2O_3.

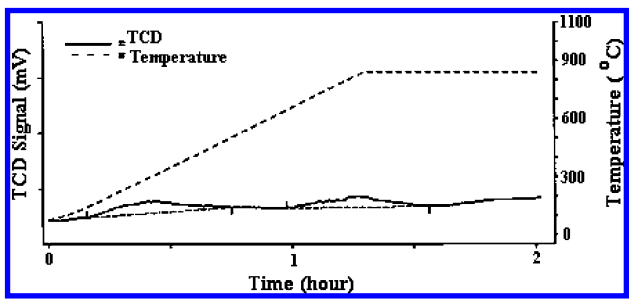

Figure 2. NH_3-TPD spectra of the γ-Al_2O_3 catalyst.

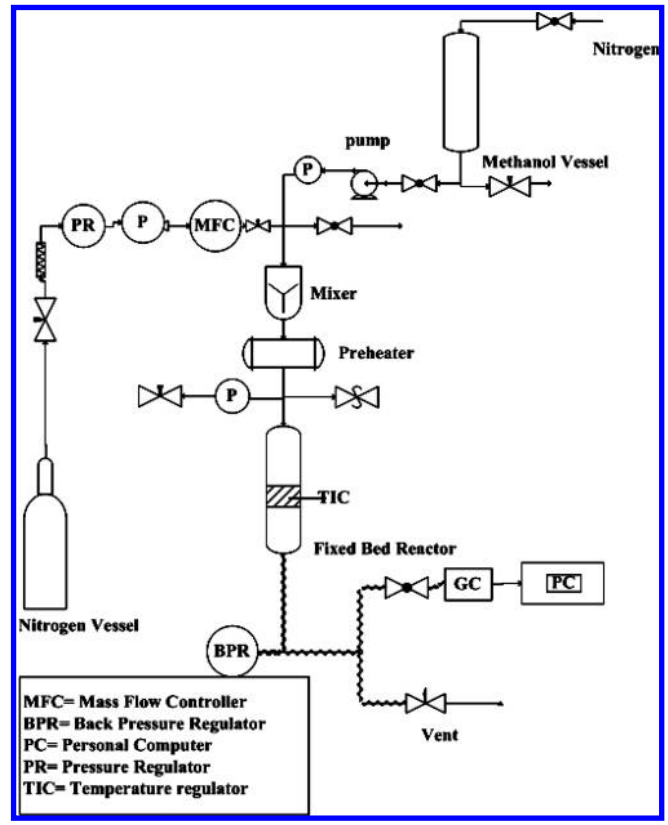

Figure 3. Schematic view of the experimental setup.

2.4. Experimental Conditions. The experiments were carried out under steady-state conditions in a fixed-bed microreactor that was composed of a stainless steel tube (i.d. $^3/_8$ in. and length 670 mm) at temperatures on the interval of 260−380 °C and pressures of 1−16 barg, assuming that the internal and external diffusion effects of the particles were eliminated. These conditions correspond to the vapor state of the reaction mixture.

In each test, 1 g of catalyst was loaded into the reactor by packing quartz wool pads at both ends of the catalyst bed, resulting in an approximate catalyst bed depth of 5 mm. The whole experiment was performed for 30 h of time on stream (TOS) after achieving steady state, and no significant deactivation was seen for 30 h of TOS.

Prior to the kinetic investigations, the initial activation of the catalyst was studied by purging N_2 in the feed section, as the internal standard, through a set of mass flow controllers (EL-FLOW; Bronkhorst High-Tech, Ruurlo, The Netherlands) and MeOH was pumped from a feed tank through a set of mini-metering pumps (Ilshin Autoclave Co., Ltd., Daejeon, Korea). MeOH and N_2 were subsequently introduced into a preheater that was set at a temperature of 523 K. The temperature of the downline effluent was constantly maintained at temperatures above 423 K, to avoid the possible condensation of water, MeOH, or DME.

A portion of the effluent gas was directed to a gas chromatograph apparatus (HP, Agilent Technologies, model HP-6890N using a HP-Plot Q column) connected online to the system in order to separate DME, MeOH, etc. The effluent gas was analyzed several times at 30 min intervals during each experimental run. The schematic view of the experimental setup is shown in Figure 3.

2.5. Kinetic Investigations. 2.5.1. Assessment of External and Internal Transfer Resistances. It is essential to examine film resistance in the particle macropores because the controlling

Table 2. Results for the Experiments Performed To Evaluate Macropore Gas-Phase Film Resistance[a]

particle size (mm)	injection number	conversion (%)
1−2	1	89.33
	2	89.68
	3	90.15
	4	87.93
	5	89.11
0.09−0.125	1	88.48
	2	86.97
	3	88.46
	4	87.49
	5	87.8

[a] Reaction conditions: $T = 300$ °C, $P = 16$ bar, and WHSV $= 26.07$ h^{-1}.

Table 3. Parameters and Their Levels

parameter	level of the parameter 1	2	3
T (°C)	260	320	380
P (barg)	1	8	16
wt % of water in the feed	0	10	20

reaction rate must not be dependent on the length of the macropores and the size of the particles. When a series of experiments with different catalyst particle sizes and constant process parameters were performed, it was found that at mesh sizes of 90−125 μm there was no macropore film resistance (Table 2).

Similarly, to check for external bulk gas-phase film resistance, a series of experiments were run. The feed flow rate was changed, with a corresponding change in the catalyst loading, so that a constant space velocity was achieved. On the basis of the experimental results, it is observed that the points that correspond to the same WHSV but differ in flow rates are close together. Accordingly, it may be certainly stated that film resistance in the bulk gas phase does not control the total reaction rate for the 0.1 mm catalyst particles.

2.5.2. Experimental Design. To design the kinetic experiments, a full factorial method was implemented because factorial designs allow the effects of a factor to be estimated at several levels of the other factors, yielding conclusions that are valid over a range of experimental conditions. Furthermore, a factorial design is necessary when interactions may be present to avoid misleading conclusions.[18] In order to apply this method, the pertinent parameters of the kinetic tests, including temperature, pressure, and weight percent of water in the feed, have been considered on the kinetics of a commercial γ-Al_2O_3 catalyst in the MeOH dehydration process. In accordance with the full factorial design, for three parameters with three levels, an L-27 configuration must be considered. Table 3 shows the arrangements of the parameters and the related levels.

2.5.3. Kinetic Study. After the catalyst screening test program, kinetic experiments were conducted with mixtures of MeOH, water, and N_2 in a temperature range of 533−653 K and a pressure range of 1−16 barg. The MeOH flow rate was 0.58 mL/min in the whole experiments for the purpose of maintaining the conversion in a differential reactor at sufficiently low levels (less than 12%). Therefore, the mass of the catalyst was varied between 0.096 and 0.0005 g.

It is noted that, in each experiment, fresh catalysts were loaded to avoid the effect of deactivation. In a typical experiment, each catalyst was diluted with about 0.1−0.25 g of silicon carbide in order to achieve isothermal conditions in the catalytic bed. Also, a plug-flow regime was assumed for the gaseous feed and the contribution of axial mixing to the mass transport was neglected, considering that the ratio of the catalyst bed to the particle diameter is relatively high for all experiments.

Table 4. Experimental Conditions and Reactor Results

temperature (°C)	pressure (barg)	wt % of water in the feed	reaction rate (mol/kg·s)	DME yield (%)
260	1	0	0.0022	3.12
320	1	0	0.0049	5.31
380	1	0	0.0071	7.44
260	8	0	0.0027	3.79
320	8	0	0.0053	5.70
380	8	0	0.0073	7.62
260	16	0	0.0034	3.92
320	16	0	0.0056	5.94
380	16	0	0.0090	9.27
260	1	10	0.0013	1.90
320	1	10	0.0058	6.26
380	1	10	0.0076	7.95
260	8	10	0.0016	2.14
320	8	10	0.0062	6.56
380	8	10	0.0079	8.17
260	16	10	0.0019	2.60
320	16	10	0.0064	6.83
380	16	10	0.0086	8.57
260	1	20	0.0010	1.43
320	1	20	0.0038	4.22
380	1	20	0.0065	7.14
260	8	20	0.0012	1.68
320	8	20	0.0042	4.76
380	8	20	0.0068	7.30
260	16	20	0.0021	2.92
320	16	20	0.0046	4.97
380	16	20	0.0082	8.43

In addition, use of the following simple relationship for calculation of the reaction rate from conversion values is justified:

$$(-r_{MeOH})_{ave} = \frac{F_{MeOH}X}{W} \tag{2}$$

where $(-r_{MeOH})_{ave}$ is the average reaction rate (mol/g·min), F_{MeOH} is the initial total feed rate (mol/min), X is the fractional conversion of MeOH, and W is the weight of the catalyst (g). The yield value and experimental rate are reported in Table 4.

3. Overview of the ANNs

The ANN is a powerful mathematical modeling tool especially for complex systems. It is composed of simple computational units, called neurons, that are connected in a parallel structure. These units are inspired by biological neurons in the human brain. ANNs have been applied successfully in different areas such as function approximation and pattern recognition.

There are many kinds of ANNs introduced by researchers such as a multilayer feed forward network, a radial basis function network, a self-organizing map, and an autoasso-

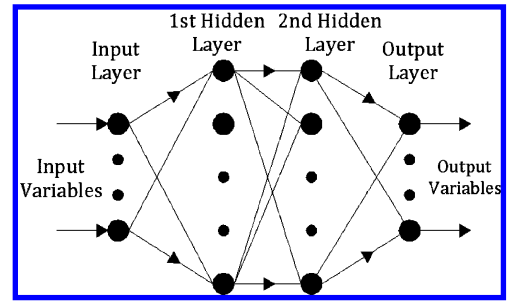

Figure 4. Structure of a typical multilayer feed forward neural network.

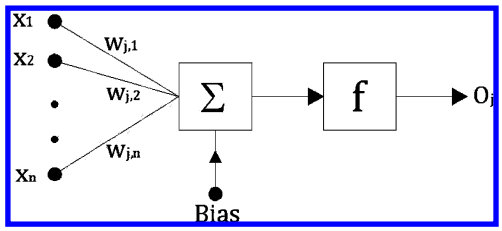

Figure 5. Structure of a simple neuron.

ciative network. One of the most commonly used neural networks is the multilayer feed forward neural network, whose structure is shown in Figure 4. Because the multilayer feed forward neural network is the most commonly used network for the function approximation problem as well as its strong learning capability, it has been used in this study. This type of network is able to approximate almost all kinds of functions regardless of their complexities.

As seen in Figure 4, a multilayer feed forward neural network has a layered structure. It usually contains an input layer, some hidden layers, and an output layer. The input variables are fed to the input layer. No processing takes place in the input layer. The variables then pass to the hidden layer(s), where processing takes place. Finally, the output of the last hidden layer is sent to the output layer. Each layer consists of some neurons whose input is the output of the previous layer's neurons.

In each neuron, the input vector was multiplied by the parameters called weight and then added with a scalar parameter called bias. This sum is fed to the differentiable function called a transfer or activation function, and finally the neuron's output can be obtained from eq 3:

$$O_j = f(w_{ji}x_i + b_j) \tag{3}$$

where O_j is the output of the jth neuron, f is the transfer or activation function, b_j is the bias of the jth neuron, w_{ji} is the synaptic weight corresponding to the ith input of the jth neuron, x_i is the ith input signal to the j^{th} neuron, and n is the number of input signals to the jth neuron.

The structure of a simple neuron can be seen in Figure 5. The most commonly used transfer functions are the sigmoid, hyperbolic tangent, and linear functions.

The neural network can be interpreted as a form of an input/output model.[19] It operates like a "black box" model, requiring no detailed information about the system,[20] and does not need an explicit formulation of the mathematical equations governing the system under study.

In order to prepare a network for a special task, the synaptic weights and biases should be adjusted. This process is called training, in which the connection weights are modified using a suitable learning algorithm. In the training process, an input is presented to the network along with its desired or target output. After the input data are introduced to the network, the corresponding output is calculated, and then the difference between the network output and the desired output is used for adjustment of the network's synaptic weights.

If there is a difference, the connection weights are altered to decrease the training error. The process continues until the training error is lower than the acceptable value. Usually the mean square error (MSE) is used as a criterion for the training error, which is defined as follows:

$$\mathrm{MSE} = \frac{1}{P}\sum_{p=1}^{P}(d_p - o_p)^2 \tag{4}$$

Table 5. Minima and Maxima of ANN Input Data

Property	min	max
temperature (°C)	260	380
pressure (barg)	1	16
purity of the feed (%)	0.8	1

Table 6. Statistical Values for Predictions of the Reaction Rate Using Various Algorithms

	hidden layer	MSE		AARE		
algorithm	neurons	training	test	training	test	R^2 (test)
LM	6	1.48×10^{-8}	6.28×10^{-7}	4.43	7.231	0.956
LM	7	1.27×10^{-8}	8.70×10^{-8}	3.85	7.86	0.997
LM	8	7.90×10^{-8}	9.98×10^{-8}	2.94	7.07	0.997
LM	9	4.95×10^{-8}	8.43×10^{-8}	3.06	7.43	0.994
LM	10	1.63×10^{-7}	2.02×10^{-7}	2.76	5.69	0.982
LM	11	2.30×10^{-8}	5.81×10^{-7}	3.13	7.31	0.940
BR	6	6.15×10^{-8}	8.89×10^{-8}	4.44	4.74	0.992
BR	7	5.88×10^{-8}	1.06×10^{-7}	4.47	4.96	0.993
BR	8	7.34×10^{-8}	9.21×10^{-8}	4.49	4.79	0.991
BR	9	3.87×10^{-9}	2.90×10^{-7}	2.80	4.85	0.977
BR	10	4.81×10^{-9}	3.02×10^{-7}	2.98	5.46	0.990
BR	11	3.07×10^{-8}	1.91×10^{-7}	3.93	4.86	0.984
SCG	6	4.93×10^{-8}	5.42×10^{-7}	6.48	8.74	0.964
SCG	7	1.52×10^{-8}	1.08×10^{-7}	3.66	4.72	0.991
SCG	8	1.58×10^{-8}	1.70×10^{-7}	3.92	4.93	0.975
SCG	9	1.55×10^{-8}	6.71×10^{-8}	3.45	6.43	0.996
SCG	10	1.53×10^{-8}	6.75×10^{-8}	3.74	7.68	0.993
SCG	11	1.59×10^{-8}	2.27×10^{-7}	4.73	9.02	0.979
GDA	6	1.60×10^{-8}	1.87×10^{-7}	8.87	8.87	0.993
GDA	7	1.60×10^{-8}	4.97×10^{-8}	7.31	7.31	0.996
GDA	8	1.59×10^{-8}	1.21×10^{-7}	2.98	4.39	0.993
GDA	9	1.60×10^{-8}	4.28×10^{-7}	6.03	9.50	0.960
GDA	10	1.60×10^{-8}	5.12×10^{-7}	3.61	7.15	0.909
GDA	11	1.58×10^{-8}	6.85×10^{-7}	5.17	8.99	0.911

where d_p and o_p are the desired and calculated outputs, respectively, for the pth training data and P is the total number of training data.

One of the most important problems in creating a neural network is selection of the proper number of hidden layers and their neurons. For the input and output layers, the number of neurons is determined by the number of input and output variables, respectively.

A network that has only one hidden layer is able to approximate almost any type of nonlinear mapping.[21] However, determination of the appropriate number of neurons for the hidden layer is difficult and is often done by trial and error.

Of course, there are some heuristics to estimate the number of hidden layer neurons. For example, the empirical formula suggested in ref 20 is as follows:

$$\mathrm{NH} = \frac{\mathrm{NI} + \mathrm{NO}}{2} + \sqrt{\mathrm{NTP}} \tag{5}$$

where NH, NI, and NO are the number of neurons for hidden, input, and output layers, respectively, and NTP is the number of training patterns.

One of the problems that may occur during neural network training is "overfitting", in which the training error has a very small value but the error of new data, which are not present in the training data set, is unacceptably large. In other words, the network has memorized the training data, but it has not learned to generalize them.[19]

In order to avoid overfitting and be ensured of the generalization ability of the neural network, the training data set has been divided into two subsets including the training and test data set. The earlier one is used to train the network, and the later is used to examine the accuracy of the network and compare the performances of various network structures.

The most commonly used algorithm to minimize the error during neural network training and obtain the optimum value

of network weights and biases is error back-propagation (EBP) in which the weights and biases are updated in the direction of the negative gradient of the training error. Other variants of EBP are also introduced such as the scaled conjugate gradient (SCG), Levenberg−Marquardt (LM), and gradient descent with momentum (GDA).

4. Application of ANNs for Estimation of the Reaction Rate in MeOH Dehydration

In order to obtain the kinetic model for DME synthesis, a multilayer feed forward neural network with one hidden layer has been used. Four different training algorithms including trainbr, trainlm, trainscg, and traingda have been used in the MATLAB platform to train and test the ANN.

The input layer of the network contains three units representing the input data that are possible factors controlling the catalyst reaction rate, i.e., temperature, pressure, and purity of the feed stream in this case. The output layer contains one unit representing the output data to be estimated, i.e., the reaction rate of DME synthesis. These input−output data were collected from 27 runs of the experimental setup. Table 5 shows the range of input data. It has to be mentioned that two-thirds of all training data are used for training and the rest are used for testing of the generalization of the network. All input and output variables have been normalized in the interval of (−1, 1).

According to eq 5, the number of hidden layer neurons is rounded to 7, although the number of the hidden layer neurons is systematically varied in the range of 6−11 to obtain the best ANN structure for estimating the training data. The tangent hyperbolic and linear functions were used as transfer functions in hidden and output layers, respectively.

The criterion for selection of the optimum ANN structure is the MSE of the test data as well as the correlation coefficient (R^2) and absolute average relative error (AARE), which are defined by eqs 6 and 7, respectively.

$$R^2 = 1 - \frac{\sum_{p=1}^{P}(d_p - o_p)^2}{\sum_{p=1}^{P}(o_p)^2} \tag{6}$$

$$\mathrm{AARE} = \frac{1}{P}\sum_{p=1}^{P}\left|\left(\frac{o_p - d_p}{d_p}\right)\right| \times 100 \tag{7}$$

5. Results and Discussion

After collection of the data set, the network was trained with different learning algorithms and different hidden layer neurons to obtain the best ANN structure. For each case, more than 50 runs of the test were conducted by changing the initial weights of the connections. Generally speaking, the estimated values were reproduced within a reasonable error. The estimated results shown here are those of minimum errors.

Table 5 summarizes the statistical values for both the training and test data. According to Table 6, Bayesian regularization (BR) and SCG show less prediction error than the other two algorithms.

As can be seen, the SCG with seven hidden layer neurons has the minimum AARE for the test data, with a value of 4.72%. Their corresponding MSE and R^2 values in testing are 1.08×10^{-7} and 0.991, respectively.

The best result for the BR algorithm corresponds to six hidden layer neurons with AARE in testing equal to 4.74% and MSE and R^2 equal to 8.89×10^{-8} and 0.992.

Plots of AARE versus the number of hidden layer neurons for different training algorithms are shown in Figure 6. As can be seen, the optimum numbers of hidden layer neurons for LM, BR, SCG, and GDA are 10, 6, 7, and 8, respectively.

The experimental and predicted results for test data for the optimum number of hidden layer neurons are shown in Figure 7. As can be seen, the experimental and predicted results are

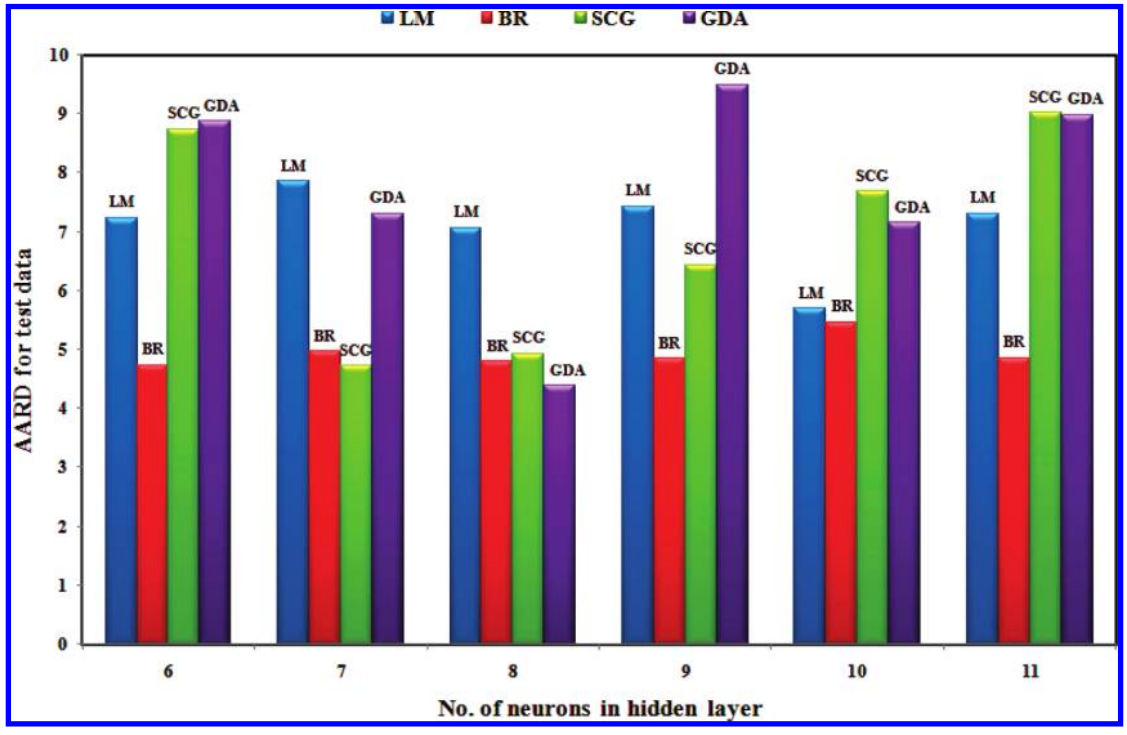

Figure 6. AARE versus the number of hidden layer neurons for different algorithms.

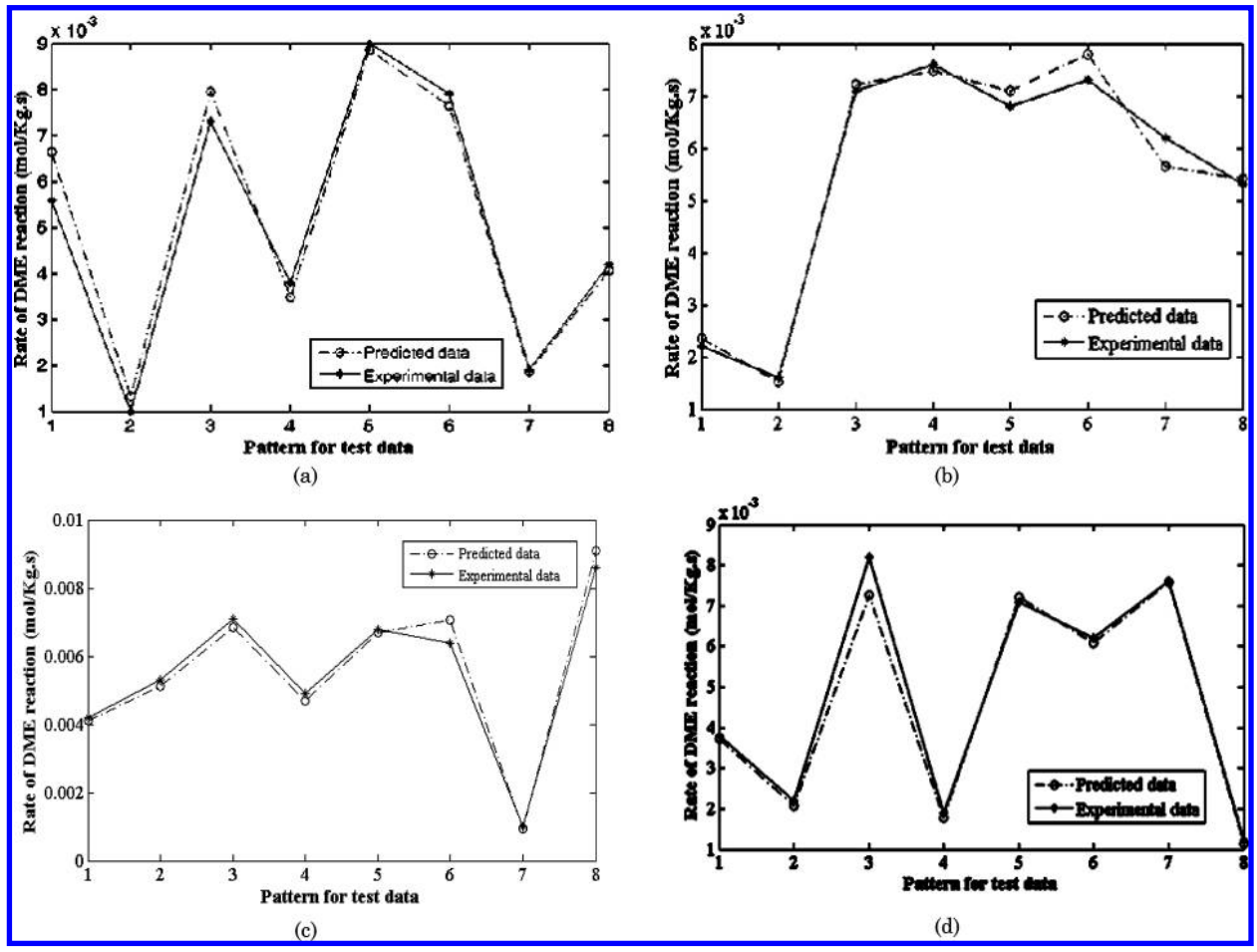

Figure 7. Comparison of the experimental and predicted results for different algorithms with the optimum number of neurons in the hidden layer: (a) LM; (b) BR; (c) SCG; (d) GDA.

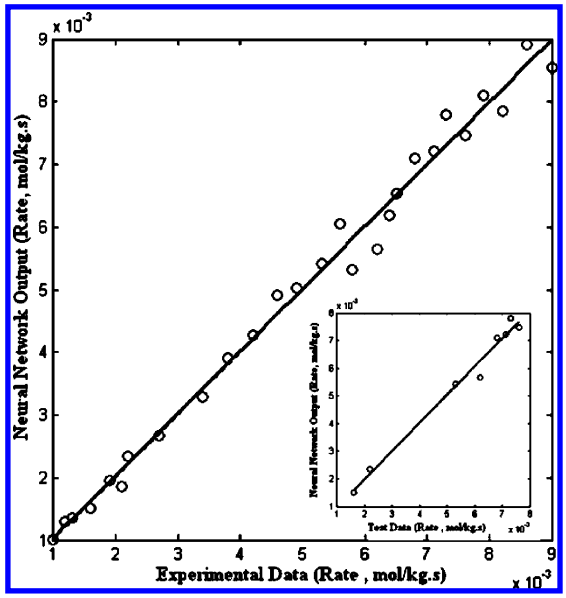

Figure 8. Predicted results versus experimental data for the BR algorithm with six neurons in the hidden layer.

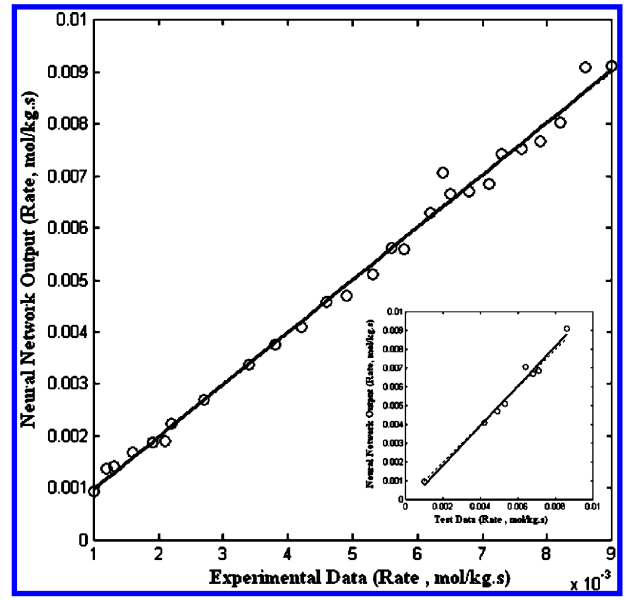

Figure 9. Predicted results versus experimental data for the SCG algorithm with seven neurons in the hidden layer.

very close to each other, and for some data test patterns, two lines, shown in Figure 7, are almost indistinguishable.

Figures 8 and 9 present the predicted results by neural network versus experimental data for both all data sets and test data, for the two selected BR and SCG algorithms with the optimum number of hidden layer neurons. They indicate the good accuracy of the neural network to estimate the reaction rate in MeOH dehydration. From the results shown in Table 6, the R^2 values for the optimum number of hidden layer neurons are very close to unity, proving a reasonably good quality of the fit for our experimental data by the ANN. It is noted that the values predicted by the ANN have a better agreement with

experimental data than classic kinetic modeling results by previous researches in open literature.[4,13,22]

6. Conclusion

In this paper, the ability of the neural network to estimate the reaction rate of MeOH dehydration was examined. The obtained results led to the conclusion that the estimated values agreed very well with the experimental values, even in the case where the experimental data seemed to contain some experimental error.

This study indicates that values predicted by the ANN have better agreement with experimental data than classic kinetic modeling results by previous researchers. The capability of learning from experimental data and simplicity of implementation are the advantages of the ANNs over the classic kinetic modeling methods. According to this simulation, the results infer high capability of the ANN for simulation of MeOH dehydration reactions.

Acknowledgment

The authors acknowledge financial support of this work by research and technology affairs of the National Iranian Petrochemical Company.

Literature Cited

(1) Nie, Z.; Liu, H.; Liu, D. W.; Fang, D. Intrinsic kinetics of dimethyl ether synthesis from syngas. *J. Nat. Gas Chem.* **2005**, *14*, 22.

(2) Moradi, G. R.; Ahmadpour, J.; Yaripour, F. Intrinsic kinetics study of LPDME process from syngas over bifunctional catalyst. *Chem. Eng. J.* **2008**, *144*, 88.

(3) Mollavali, M.; Yaripour, F.; Atashi, H.; Sahebdelfar, S. Intrinsic kinetics study of dimethyl ether synthesis from methanol on γ-Al_2O_3 catalysts. *Ind. Eng. Chem. Res.* **2008**, *47*, 3265.

(4) Pop, G.; Bozga, G.; Ganea, R.; Natu, N. Methanol conversion to dimethyl ether over H-SAPO-34 catalyst. *Ind. Eng. Chem. Res.* **2009**, *48*, 7065.

(5) Kim, J. H.; Park, M. J.; Kim, S. J.; Joo, O. S.; Jung, K. D. DME synthesis from synthesis gas on the admixed catalysts of Cu/ZnO/Al_2O_3 and ZSM-5. *Appl. Catal., A* **2004**, *264*, 37.

(6) Topp-Jorgensen, J. Process for the preparation of catalysts for use in ether synthesis. U.S. Patent 4,536,485, 1985.

(7) Bercic, G.; Levec, J. Intrinsic and global reaction rate of methanol dehydration over γ-Al_2O_3 pellets. *Ind. Eng. Chem. Res.* **1992**, *31*, 1035.

(8) Bandiera, J.; Naccache, C. Kinetics of methanol dehydration on dealuminated H-mordenite: model with acid and basic active centers. *Appl. Catal., A* **1991**, *69*, 139.

(9) An, W.; Chuang, K. T.; Sanger, A. Dehydration of methanol to dimethyl ether by catalytic distillation. *Can. J. Chem. Eng.* **2004**, *82*, 948.

(10) Al Wahabi, S. M. Conversion of methanol to light olefins on SAPO-34, kinetic modeling and reactor design. Ph.D. Dissertation, Texas A&M University, College Station, TX, 2003.

(11) Lu, W.; Teng, L.; Xiao, W. Simulation and experiment study of dimethyl ether synthesis from syngas in a fluidized-bed reactor. *Chem. Eng. Sci.* **2004**, *59*, 5455.

(12) Bercic, G.; Levec, J. Catalytic dehydration of methanol to dimethyl ether, kinetic investigation and reactor simulation. *Ind. Eng. Chem. Res.* **1993**, *32*, 2478.

(13) Lee, E.; Park, Y.; Joo, O.; Jung, K. Methanol dehydration to produce dimethyl ether over γ-Al_2O_3. *React. Kinet. Catal. Lett.* **2006**, *89* (1), 115.

(14) Yaripour, F.; Mollavali, M.; Mohammadi Jam, Sh.; Atashi, H. Catalytic dehydration of methanol to dimethyl ether catalyzed by aluminum phosphate catalysts. *Energy Fuels* **2009**, *23*, 1896.

(15) Yaripour, F.; Baghaei, F.; Schmidt, I.; Perregaard, J. Catalytic dehydration of methanol to dimethyl ether (DME) over solid-acid catalysts. *Catal. Commun.* **2005**, *6*, 147.

(16) Khom-in, J.; Praserthdam, P.; Panpranot, J.; Mekasuwandumrong, O. Dehydration of methanol to dimethyl ether over nanocrystalline Al_2O_3 with mixed γ- and χ-crystalline phases. *Catal. Commun.* **2008**, *9*, 1955.

(17) Arena, F.; Dario, R.; Pamalina, A. A characterization study of the surface acidity of solid catalysts by temperature programmed methods. *Appl. Catal., A* **1998**, *170* (1), 127.

(18) Montgomery, D. C. *Design and analysis of experiments*; John Wiley & Sons: New York, 2001; Vol. 5, p 175.

(19) Boozarjomehry, R. B.; Abdolahi, F.; Moosavian, M. A. Characterization of basic properties for pure substances and petroleum fractions by neural network. *Fluid Phase Equilib.* **2005**, *231*, 188.

(20) Kalogirou, S. A.; Bojic, M. Artificial neural networks for the prediction of the energy consumption of a passive solar building. *Energy (Amsterdam, Neth.)* **2000**, *25*, 479.

(21) Cybenko, G. Approximation by superposition's of a sigmoidal function. *Math. Control Signals Syst.* **1989**, *2* (4), 303.

(22) Hadipour, A.; Sohrabi, M. Kinetic parameters and dynamic modeling of a reactor for direct conversion of synthesis gas to dimethyl ether. *Ind. Eng. Chem. Res.* **2007**, *13* (4), 558.

Received for review December 30, 2009
Revised manuscript received March 17, 2010
Accepted March 25, 2010

IE9020705